Kinetic Analysis of a Model for Double Substrate Cycling: Highly Amplified ADP (and/or ATP) Quantification

Edelmira Valero,* Ramón Varón,* and Francisco García-Carmona†
*Grupo de Modelización en Bioquímica, Departamento de Química-Física, Escuela Politécnica Superior de Albacete, Universidad de Castilla-La Mancha, Albacete, Spain; and †Departamento de Bioquímica y Biología Molecular A, Facultad de Biología, Universidad de Murcia, Murcia, Spain

ABSTRACT A mathematical description has been made of an enzyme amplification mechanism involving the coupling of two substrate cycles. In this amplification system one of the noncycling products of a first substrate cycle acts as a trigger molecule that continuously feeds a second substrate cycle. Time-concentration equations describing the evolution of the species involved in the system have been obtained. The model is illustrated by the quantification of nanomolar levels of ADP (and/or ATP) in a continuous assay involving the enzymes L-lactate dehydrogenase and L-lactate oxidase to cycle the pyruvate accumulated in a first enzymatic cycle constituted by the enzymes pyruvate kinase and hexokinase. Progress curves were seen to be parabolic, and, according to the kinetic equations obtained, followed second-order polynomials of the reaction time. Mathematical equations for minimizing the cost of the assays are also given. The model is applicable to the amplified analytical determination of low levels of a metabolite or an enzyme activity, and its amplification capacity, together with the simplicity of determining kinetic parameters, enable it to be employed in enzyme immunoassays to increase the magnitude of the measured response.

INTRODUCTION

Substrate cycles are a biochemical mechanism in living organisms that amplify and speed up the response against a weak stimulus (Newsholme et al., 1984). In the reaction scheme described, an enzyme catalyzing a reaction in a given way inside a metabolic pathway is opposed by another enzyme catalyzing the reaction in the opposite direction, in such a way that the product of the reaction catalyzed by the first enzyme is a substrate of the second enzyme and vice versa. Concurrent flux through these opposing reactions, which are catalyzed far from equilibrium by two different enzymes, uses chemical energy (usually the hydrolysis of ATP) with no net conversion of the recycling substrate to product. Thus substrate cycles were initially so-called futile cycles because of the apparent lack of a biochemical function, although potential roles in thermogenesis and metabolic regulation have since been suggested (Newsholme, 1978; Newsholme et al., 1984; Hammond and Johnston, 1987; Ibarguren et al., 2000).

Substrate cycles constitute an example of an in vivo biological response amplification system applied for in vitro purposes. Their great sensitivity has been applied to the quantitative determination of low levels of a metabolite or to the amplification of an enzymatic activity by coupling two bisubstrate enzyme-catalyzed reactions acting in opposite directions (Passonneau and Lowry, 1978, 1993). Thus, this type of reaction scheme has been used in enzyme-linked immunoassays (Harper and Orengo, 1981; Johannsson et al., 1986; Inouye et al., 2002) and has been implemented in a double bioreactor cell using immobilized enzymes (Raba and Mottola, 1994). Kinetic analyses of these systems have been reported in both the steady state (Passonneau and Lowry, 1978) and the transient phase (Valero and García-Carmona, 1998; Valero et al., 2000), and equations have been obtained for calculating enzyme quantities that minimize the cost of assays (Valero and García-Carmona, 1996) as well as for measuring low levels of an enzyme activity by coupling it to a substrate cycle in a continuous assay (Valero et al., 1995, 1997).

Sensitivity can be increased even further by double-cycling. In this amplification approach one of the noncycling products of a first substrate cycle acts as a trigger molecule that feeds a second substrate cycle (Scheme 1). This procedure has been applied to measuring nanomolar levels of NADP-NADPH and ADP-ATP (Passonneau and Lowry, 1993), although always in discontinuous assays. This fact, together with the absence of time-based equations that would make it possible to follow the process in a continuous form, led us to solve the corresponding set of differential equations. In this study, our goal was therefore to develop kinetic equations describing the time-dependence of species involved in Scheme 1. The model is experimentally illustrated by measuring ADP (and/or ATP) in a continuous assay via the coupling of pyruvate kinase (EC 2.7.1.40) and hexokinase (EC 2.7.1.1), using the enzymes L-lactate dehydrogenase (EC 1.1.1.27) and L-lactate oxidase (EC 1.1.3.*x*; *x* to be determined) (Naka, 1993), to cycle the pyruvate accumulated in the first enzymatic cycle.

Submitted October 15, 2003, and accepted for publication January 23, 2004.

Address reprint requests to Edelmira Valero, Grupo de Modelización en Bioquímica, Departamento de Química-Física, Escuela Politécnica Superior de Albacete, Universidad de Castilla-La Mancha, Campus Universitario, E-02071-Albacete, Spain. Tel.: 34-967-59-9200; Fax: 34-967-59-9224; E-mail: edelmira.valero@uclm.es.

0006-3495/04/06/3598/09 $2.00

doi: 10.1529/biophysj.103.035956

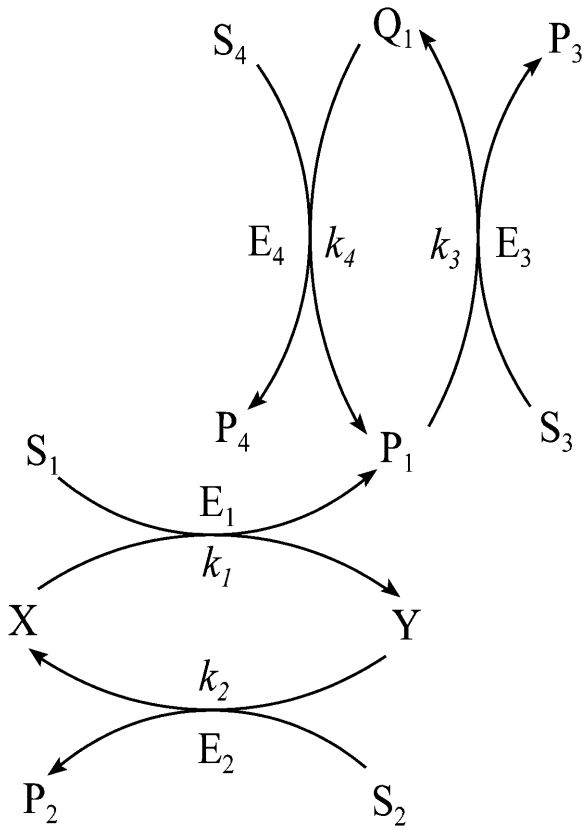

SCHEME 1 Reaction scheme proposed for double-cycling assays. One of the noncycling products accumulated in a first substrate cycle, P_1, continuously feeds a second substrate cycle, where it is sequentially interconverted into Q_1.

MATERIALS AND METHODS

Reagents

Beta-NADH, ADP, D-(+)-glucose, sodium phosphoenolpyruvate, sodium pyruvate, BSA, pyruvate kinase (490 units mg^{-1}) from chicken muscle, hexokinase (238 units mg^{-1}) from Bakers yeast, L-lactate dehydrogenase (544 units mg^{-1}) from chicken heart, and L-lactate oxidase (39 units mg^{-1}) from *Pediococcus* species were obtained from Sigma (Madrid, Spain). Stock solutions of enzymes (36.3, 35.7, 72.9, and 100 units ml^{-1}, respectively) were prepared in 50 mM Tris/acetic acid buffer (pH 7.5) containing 1 mg ml^{-1} BSA, and further dialyzed at 4°C against this buffer (in the absence of BSA) to decrease the presence of contaminants. All other reagents were of analytical grade and were used without further purification. All solutions were prepared in ultrapure deionized nonpyrogenic water.

Methods

Spectrophotometric readings were obtained on a Uvikon XS from Bio-Tek Instruments (Winooski, VT). The temperature was maintained at 37°C using a Hetofrig Selecta (Barcelona, Spain) circulating bath with a heater/cooler and checked using a Cole-Parmer (Vernon Hill, IL) digital thermometer with a precision of ±0.1°C.

Cycling assay for ADP

This method was used to evaluate the general rate constant of the first cycle, k_{1c}, as well as the presence of ADP and/or ATP as contaminants in the reaction medium. The standard reaction mixture consisted of 281.6 μM β-NADH, 2 mM phosphoenolpyruvate, 75 mM potassium acetate, 2 mM magnesium chloride, 3 mM glucose, 1.8 units of hexokinase, 1.8 units of pyruvate kinase, 14.8 units of L-lactate dehydrogenase, and different volumes of a stock solution of 10 μM ADP, in 50 mM Tris/acetic acid buffer (pH 7.5). The apparent first-order rate constants k_1 and k_2 were also determined by this method, performing a set of experiments by varying the concentration of one enzyme while maintaining the concentration of the other fixed, using an initial concentration of ADP of 1 μM, as previously described (Valero et al., 1995; Valero and García-Carmona, 1996). The reaction was started by the addition of pyruvate kinase, the final volume being 0.5 ml. The time course of the reaction was followed by measuring the disappearance of β-NADH at 340 nm ($NADH_{340}$ = 6270 M^{-1} cm^{-1}) at 37°C.

The experimental progress curves thus obtained were fitted by linear regression to a first-order polynomial equation of the reaction time using the SigmaPlot Scientific Graphing System version 8.0 (2002, SPSS, Chicago, IL).

Cycling assay for pyruvate

This method was used to evaluate the general rate constant of the second cycle, k_{2c}, as well as the presence of pyruvate and/or L-lactate as contaminants in the reaction medium. The standard reaction mixture consisted of 256 μM β-NADH, 75 mM potassium acetate, 2 mM magnesium chloride, 2.2 units of L-lactate dehydrogenase, 3 units of L-lactate oxidase, and different volumes of a stock solution of 10 μM pyruvate, in 50 mM Tris/acetic acid buffer (pH 7.5). The apparent first-order rate constants k_3 and k_4 were also determined by this method, performing a set of experiments by varying the concentration of one enzyme while maintaining the concentration of the other fixed, using an initial concentration of pyruvate of 1 μM, as previously described (Valero et al., 1995; Valero and García-Carmona, 1996). The reaction was started by the addition of L-lactate dehydrogenase, the final volume being 0.5 ml. The time course of the reaction was followed by measuring the disappearance of β-NADH at 340 nm at 37°C.

The experimental progress curves obtained were fitted by linear regression to a first-order polynomial equation of the reaction time as previously indicated.

Double-cycling assay for ADP

The cycling reagent contained the following final concentrations: 281.6 μM β-NADH, 2 mM phosphoenolpyruvate, 75 mM potassium acetate, 2 mM magnesium chloride, 3 mM glucose, 1.8 units of hexokinase, 3 units of L-lactate oxidase, 2.2 units of L-lactate dehydrogenase, 1.8 units of pyruvate kinase, and different volumes of a stock solution of 500 nM ADP, in 50 mM Tris/acetic acid buffer (pH 7.5). The reaction was started by the addition of pyruvate kinase, the final volume being 0.5 ml. The time course of the reaction was followed by measuring the disappearance of β-NADH at 340 nm at 37°C.

The resulting experimental progress curves were fitted by linear regression to a second-order polynomial equation of the reaction time, as previously indicated.

KINETIC ANALYSIS

The reaction mechanism shown in Scheme 1 corresponds to the simultaneous coupling of two substrate cycles. One of the noncycling products of a first substrate cycle between the metabolites X and Y (we will consider P_1 but the equations corresponding to P_2 can be obtained in the same way) continuously feeds a second substrate cycle, where it is

sequentially interconverted into another metabolite (Q_1), without being consumed. The reaction velocity of the second substrate cycle continuously increases, since the system is continuously injecting substrate into it. Under these conditions, a very small quantity of P_1 synthesized from the first substrate cycle can catalyze the formation of large quantities of the products P_3 and P_4, and thus the system acts as a chemical amplifier in the quantitative determination of X and/or Y.

To derive analytical equations for the time dependence of species involved in Scheme 1 the following assumptions, which can be easily implemented in experimental conditions, were made:

1. Nonrecycling substrates concentrations, $[S_i]$ ($i = 1,2,3,4$), are high enough to be saturating or remain constant during the reaction time.
2. During cycling, the concentration of recycling substrates, $[X]$, $[Y]$, $[P_1]$, and $[Q_1]$, must be clearly lower than their respective Michaelis-Menten constants ($K_{m,i}$ toward E_i ($i = 1,2,3,4$), respectively), so that the reaction rates of the four steps remain of the first order with respect to their concentrations.

In these conditions, the differential equation system that describes the reaction Scheme 1 is

$$d[X]/dt = -k_1[X] + k_2[Y] \tag{1}$$

$$d[Y]/dt = k_1[X] - k_2[Y] \tag{2}$$

$$d[Q_1]/dt = k_3[P_1] - k_4[Q_1] \tag{3}$$

$$d[P_1]/dt = k_1[X] - k_3[P_1] + k_4[Q_1] \tag{4}$$

$$d[P_2]/dt = k_2[Y] \tag{5}$$

$$d[P_3]/dt = k_3[P_1] \tag{6}$$

$$d[P_4]/dt = k_4[Q_1], \tag{7}$$

where k_i ($i = 1,2,3,4$) are apparent first-order rate constants, and $k_i = V_{max}/K_{m,i}$, where V_{max} is the reaction rate of step i at saturating concentrations of both substrates; $K_{m,i}$ is a function of the Michaelis-Menten constants of the enzyme E_i toward its substrates and of the initial concentration of S_i, respectively, with $K_{m,i} \approx K_m^x$, K_m^y, K_m^{P1}, or K_m^{01} if the corresponding S_i is saturating.

Taking into account that $[X] = X_0$ and $[Y] = Y_0$ at $t = 0$, the solution of Eqs. 1 and 2 is given by Valero and García-Carmona (1996) as

$$[X] = \frac{k_1X_0 - k_2Y_0}{\lambda_1}e^{-\lambda_1 t} + \frac{k_2(X_0 + Y_0)}{\lambda_1} \tag{8}$$

$$[Y] = -\frac{k_1X_0 - k_2Y_0}{\lambda_1}e^{-\lambda_1 t} + \frac{k_1(X_0 + Y_0)}{\lambda_1}. \tag{9}$$

Inserting Eq. 8 into Eq. 4 and solving the differential equations system constituted by the equation thus obtained and Eq. 3, taking into account the initial conditions $[Q_1] = Q_{1,0}$ and $[P_1] = P_{1,0}$ at $t = 0$, we obtain

$$[P_1] = A_1e^{-\lambda_1 t} + A_2e^{-\lambda_2 t} + A_3t + A_4 \tag{10}$$

$$[Q_1] = B_1e^{-\lambda_1 t} + B_2e^{-\lambda_2 t} + B_3t + B_4, \tag{11}$$

where $\lambda_1$and λ_2 are given by

$$\lambda_1 = k_1 + k_2 \tag{12}$$

$$\lambda_2 = k_3 + k_4, \tag{13}$$

and the parameters A_i and B_i are defined in the Appendix (Eqs. A1–A4, and Eqs. A5–A8, respectively).

Inserting Eq. 9 into Eq. 5 and integrating again with the initial condition $[P_2] = 0$ at $t = 0$, the following expression is obtained for the time-dependence of P_2:

$$[P2] = -\frac{k_2(k_1X_0 - k_2Y_0)}{\lambda_1^2}(1 - e^{-\lambda_1 t}) + \frac{k_1k_2(X_0 + Y_0)}{\lambda_1}t. \tag{14}$$

Inserting now Eqs. 10 and 11 into Eqs. 6 and 7, respectively, and integrating again with the initial conditions $[P_3] = 0$ and $[P_4] = 0$ at $t = 0$, the following expressions are obtained:

$$[P_3] = k_3\left[\frac{A_1}{\lambda_1}(1 - e^{-\lambda_1 t}) + \frac{A_2}{\lambda_2}(1 - e^{-\lambda_2 t}) + \frac{A_3}{2}t^2 + A_4t\right] \tag{15}$$

$$[P_4] = k_4\left[\frac{B_1}{\lambda_1}(1 - e^{-\lambda_1 t}) + \frac{B_2}{\lambda_2}(1 - e^{-\lambda_2 t}) + \frac{B_3}{2}t^2 + A_4t\right]. \tag{16}$$

When the steady state is reached ($t \to \infty$), the exponential terms in Eqs. 10–11 and 14–16 may be considered negligible and, by reordering the terms, we obtain

$$[P_1]_{ss} = A_3t + A_4 \tag{17}$$

$$[Q_1]_{ss} = B_3t + B_4 \tag{18}$$

$$[P_2]_{ss} = -\frac{k_2(k_1X_0 - k_2Y_0)}{\lambda_1^2} + \frac{k_1k_2(X_0 + Y_0)}{\lambda_1} \tag{19}$$

$$[P_3]_{ss} = k_3\left(\frac{A_1}{\lambda_1} + \frac{A_2}{\lambda_2} + \frac{A_3}{2}t^2 + A_4 t\right) \quad (20)$$

$$[P_4]_{ss} = k_4\left(\frac{B_1}{\lambda_1} + \frac{B_2}{\lambda_2} + \frac{B_3}{2}t^2 + B_4 t\right). \quad (21)$$

Equations 17–19 indicate that both recycling substrates of the second cycle, P_1 and Q_1, and also P_2, are accumulated linearly in the steady state. However, Eqs. 20 and 21 reveal that both products of the second cycle, P_3 and P_4, are accumulated parabolically in the steady state, i.e., the rate of the second cyclic reaction continuously increases with time as long as the conditions assumed are fulfilled. The second derivative of Eqs. 20 and 21 with respect to time indicates this increase in the reaction rate with time allowing us to define a new kinetic parameter that remains constant during the reaction. This is the acceleration of the reaction, which is the product of the two general rate constants for the two cycles multiplied by the sum of the initial concentrations of X and Y:

$$a = \frac{k_1 k_2 k_3 k_4}{\lambda_1 \lambda_2}(X_0 + Y_0). \quad (22)$$

When $\lambda_1$and λ_2 are sufficiently high to make the exponential terms in Eqs. 10–11 and 14–16 negligible, then Eqs. 17–21 are valid from near the beginning of the reaction. One way to check this is to take the first derivative of the progress curve corresponding to P_3 or P_4 accumulation with time and to ensure that it is linear. These equations are second-order polynomials of the reaction time and so experimental data from the progress curves of either P_3 or P_4 may be easily fitted to them by linear regression for the kinetic parameters involved in the system to be evaluated.

The equations corresponding to the particular case in which the substrates of the second cycle P_1 and/or Q_1 are not present as contaminants at the start of the reaction, i.e., $P_{1,0} = 0$ and/or $Q_{1,0} = 0$, can easily be obtained from those presented here by inserting this condition into the equations. The same holds for X or Y, although one of them, at least, must be present at $t = 0$.

Economical optimization

From an analytical point of view, the most important kinetic parameter in Eqs. 20 and 21 is the acceleration of the reaction since it is linearly dependent on initial X and Y concentrations. An examination of the mathematical expression corresponding to the acceleration of the reaction (Eq. 22) reveals that the cost of a continuous double-cycling assay can be minimalized by taking into account the cost of each single substrate cycle involved in the system and its respective general rate constant k_{ic} ($i = 1,2$). To do this, we define a new parameter k as

$$k = k_{1c}k_{2c}, \quad (23)$$

where

$$k_{1c} = \frac{k_1 k_2}{k_1 + k_2} \quad (24)$$

and

$$k_{2c} = \frac{k_3 k_4}{k_3 + k_4}. \quad (25)$$

The parameter k could be designated as the general acceleration constant of the double cycle, and represents the degree of acceleration attained in the measurement per unit of concentration to be detected.

Taking k_{1c} (or k_{2c}) from Eq. 23, we obtain

$$k_{1c} = \frac{k}{k_{2c}}. \quad (26)$$

According to this equation, a graphical representation of k_{1c} versus k_{2c} will be an inverse first-order plot, whose points are all the possible combinations of k_{1c} and k_{2c}, allowing us to obtain a given k (see Fig. 4).

C_1 and C_2 being the cost per unit of general rate constant for a single-cycling assay, the cost of the double-cycling assay will be

$$Cost = C_1 k_{1c} + C_2 k_{2c}. \quad (27)$$

Substituting Eq. 26 into Eq. 27, taking partial derivatives of the cost with respect to the remaining k_{2c} value and setting the derivative equal to zero, one can resolve the values of k_{1c} and k_{2c} which give the desired degree of acceleration k but minimize cost:

$$k_{1c} = \sqrt{\frac{C_2 k}{C_1}} \quad (28)$$

$$k_{2c} = \sqrt{\frac{C_1 k}{C_2}}. \quad (29)$$

The ratio between k_{1c} and k_{2c} is

$$k_{1c} = \frac{C_2}{C_1}k_{2c}. \quad (30)$$

Therefore, a graphical representation of the values of k_{1c} versus the values of k_{2c} obtained from Eqs. 28 and 29, respectively, for different k-values, is a straight line which goes through the origin and which contains all points for the pairs of general rate constants for each single substrate cycle, with the minimum cost for each k-value being the slope of this line of the minimum cost C_2/C_1. Thus, the point of

TABLE 1 A collection of metabolites which can be estimated by double substrate cycling

	X and/or *Y*				
	ADP and/or ATP*	AMP and/or ATP†	β-NADP$^+$ and/or β-NADH‡	L-Glutamate and/or 2-oxoglutarate§	L-Lysine and/or 6-amino-2-oxo-hexanoate§
S_1	Phosphoenolpyruvate	Phosphoenolpyruvate	Isocitrate	L-Alanine	L-Aspartate
S_2	D-Glucose	Luciferin	Oxaloacetate	O_2	O_2
S_3	*β-NADH*	β-NADH	L-Alanine	*β-NADH*	*β-NADH*
S_4	O_2	*O_2*	*O_2*	O_2	O_2
P_1	Pyruvate	Pyruvate	2-Oxoglutarate	Pyruvate	Oxaloacetate
P_2	D-Glucose-6-phosphate	Oxidized luciferin	Malate	$NH_3 + H_2O_2$	$NH_3 + H_2O_2$
P_3	β-NADP$^+$	β-NADP$^+$	Pyruvate	β-NADP$^+$	β-NADP$^+$
P_4	H_2O_2	H_2O_2	*$NH_3 + H_2O_2$*	H_2O_2	H_2O_2
Q_1	L-Lactate	L-Lactate	L-Glutamate	L-Lactate	Malate
E_1	Pyruvate kinase (EC 2.7.1.40)	Pyruvate, phosphate dikinase (EC 2.7.9.1)	Isocitrate dehydrogenase (NADPH) (EC 1.1.1.41)	Alanine transaminase (EC 2.6.1.2)	Aspartate transaminase (EC 2.6.1.1)
E_2	Hexokinase (EC 2.7.1.1)	Luciferase (EC 1.13.12.7)	Malate dehydrogenase (EC 1.1.1.37)	L-Glutamate oxidase (EC 1.4.3.11)	L-Lysine oxidase (EC 1.4.3.14)
E_3	L-Lactic dehydrogenase (EC 1.1.1.27)	L-Lactic dehydrogenase (EC 1.1.1.27)	Alanine transaminase (EC 2.6.1.2)	L-Lactic dehydrogenase (EC 1.1.1.27)	Malate dehydrogenase (EC 1.1.1.37)
E_4	L-Lactate oxidase (EC 1.1.3.*x*)	L-Lactate oxidase (EC 1.1.3.*x*)	L-Glutamate oxidase (EC 1.4.3.11)	L-Lactate oxidase (EC 1.1.3.*x*)	Malate oxidase (EC 1.1.3.3)

The reactive whose measurement is recommended has been written in italics in each case.
*From Breckenridge (1964), Passonneau and Lowry (1993), Raba and Mottola (1994), Valero and García-Carmona (1996), and Valero et al. (1997).
†From Raba and Mottola (1994), Valero and García-Carmona (1996), Valero et al. (1997), and Sakakibara et al. (1999).
‡From Passonneau and Lowry (1993) and Valero et al. (1997). This assay is also valid for estimating β-NADP$^+$ and/or β-NADPH by substituting E_1 and E_2 by the specific enzymes isocitrate dehydrogenase (NADP$^+$) (EC 1.1.1.42) and/or malate dehydrogenase (NADPH) (EC 1.1.1.82), respectively.
§From Luong et al. (1991), Passonneau and Lowry (1993), Raba and Mottola (1994), Valero and García-Carmona (1996, 1998), and Valero et al. (1997). These two assays are also valid for estimating any L-amino acid and/or its corresponding 2-oxo acid by substituting E_2 by the specific L-amino acid oxidase (provided that this enzyme is available).

intersection of the curve obtained by plotting Eq. 26 after fixing k with the optimized straight line will be the coordinates of the desired optimum point (k^0_{1c} and k^0_{2c}; see Fig. 4).

In this way, the cost of a double-cycling assay has been optimized by taking into account the general rate constant of each substrate cycle involved in the system, and its price. In addition, this price can be pre-minimized by calculating the smallest amount of enzymes that should be used to obtain the desired general rate constant of each substrate cycle as previously reported (Valero and García-Carmona, 1996).

Applicability of the mathematical model

The equations here obtained are applicable to all enzyme systems that fit to the reaction mechanism shown by Scheme 1, with the only restriction that the enzymes involved in the two cycles, E_i ($i = 1,2,3,4$), must follow Michaelis-Menten kinetics so that the system is linear, since the conditions concerning to substrates concentrations depend only on the concentrations used, and on the reaction time in the case of P_1 and Q_1.

Table 1 shows different metabolites that can be analyzed by this type of method, including the identities of all components involved in the system.

RESULTS AND DISCUSSION

In this section the experimental results obtained in the continuous measurement of low levels of ADP amplified by double substrate cycling are shown, thus illustrating the validity of the proposed model and of the equations obtained. According to the notation used in the Kinetic Analysis section, X and Y are ADP and ATP, respectively; P_1 and Q_1 are pyruvate and L-lactate, respectively; S_1, S_2, S_3, and S_4 are phosphoenolpyruvate, D-glucose, β-NADH, and O_2, respectively; P_2, P_3, and P_4 are glucose-6-phosphate, β-NADP$^+$, and H_2O_2, respectively; and E_1, E_2, E_3, and E_4 are pyruvate kinase, hexokinase, L-lactic dehydrogenase, and L-lactate oxidase, respectively.

Evaluation of optimum conditions

Progress curve equation covering the whole course of the reaction in a single-cycling assay under the assumptions made here is of the form (Valero and García-Carmona, 1996)

$$[P] = \gamma(1 - e^{-\lambda t}) + \alpha t. \tag{31}$$

where λ is the sum of the apparent first-order rate constants corresponding to the two enzymes (E_i and E_j) involved in the cycle ($\lambda = k_i + k_j$), and the steady-state rate $\alpha = k_i k_j (A_0 + B_0)/(k_i + k_j)$, with A_0 and B_0 being the initial concentrations

of recycling substrates. When the steady state is reached (it may be at the onset of the reaction if λ is high enough to make the exponential term in Eq. 31 negligible), the product is accumulated linearly with time.

Thus, to evaluate the most appropriate conditions for running the synchronized double-cycling assay, we first checked, running the two substrate cycles separately as indicated in Materials and Methods, enzymes concentrations yielding linear product accumulation curves from the very beginning of the reaction, thus indicating that exponential terms in the above equation may be considered negligible. However, this fact does not necessarily mean that the sum of exponential terms in Eqs. 15 and 16 when running the corresponding double-cycling assay may be also considered negligible, since both the polynomic component in progress curve equations and the coefficients of exponential terms are different in single- and double-cycling assays. Taking into account that progress curves are parabolic, the presence of a significant transient phase previous to the steady state should be established by regression analysis, considering the chosen scale time. The duration of this lag phase depends on the rate constants of the four enzymatic steps involved in the system (k_1, k_2, k_3, and k_4), in agreement with Eqs. 12 and 13, so it will be shorter as the concentration of the four enzymes is increased.

Taking into account Assumption 1 in the Kinetic Analysis, it was also confirmed that the phosphoenolpyruvate, glucose, and β-NADH concentrations were saturating, i.e., the rate of the reaction was of zero order with respect to these reagents. Furthermore, K^+ and Mg^{2+} ions concentrations were also optimized by this means.

The general rate constant of each enzymatic cycle involved in the system, k_{ic} ($i = 1,2$), was also evaluated by running single-cycling assays at different initial recycling substrate concentrations (ADP and pyruvate, respectively). A value of $4.5 \pm 7.93 \times 10^{-2}$ min^{-1} was obtained for the pyruvate kinase/hexokinase cycle (k_{1c}), and $2.6 \pm 7.56 \times 10^{-2}$ min^{-1} for the L-lactate dehydrogenase/L-lactate oxidase cycle (k_{2c}). In addition, these experiments (data not shown) allowed us to evaluate the presence of ADP and/or ATP, and pyruvate and/or L-lactate as contaminants, obtaining a value of 48.9 ± 7.26 pmol for ADP plus ATP, and 328.3 ± 39.06 pmol of pyruvate plus L-lactate under the conditions used (Materials and Methods). Apparent first-order rate constants for each enzyme involved in the system, k_i ($i = 1,2,3,4$), were also evaluated by this method, as indicated in Materials and Methods, giving the following values: $k_1 = 1.64 \pm 0.10$, $k_2 = 1.96 \pm 0.33$, $k_3 = 1.58 \pm 0.09$, and $k_4 = 0.06 \pm 0.009$ min^{-1} per μg of enzyme, respectively.

Time course of the reaction

The time course of the double-cycling coupled reaction was followed by continuously monitoring the decrease in absorbance at 340 nm owing to the consumption of β-NADH (S_3). According to Eq. 20, the equation that describes the variation of S_3 concentration with time once the steady state has been reached is

$$[S_3]_{ss} = S_{3,0} - k_3\left(\frac{A_1}{\lambda_1} + \frac{A_2}{\lambda_2} + \frac{A_3}{2}t^2 + A_4 t\right). \quad (32)$$

Fig. 1 shows a selection of progress curves obtained experimentally for different initial concentrations of ADP under the conditions described in Materials and Methods. It can be seen that the progress of the reaction was parabolic, according to the equations here obtained. These data were therefore fitted by linear regression to second-order polynomial equations of the reaction time in accordance with Eq. 32, after a preliminary check, by taking the first derivative, that the exponential terms in Eq. 15 may be considered negligible. Taking into account Eq. 1 in the kinetic analysis, curves were registered in all cases up to an absorbance value at 340 nm of 0.32 (51 μM β-NADH), a concentration much higher than the apparent K_m^{NADH} toward L-lactate dehydrogenase ($\sim$1 μM with 3 μM pyruvate (Passonneau and Lowry, 1993). The regression coefficients thus obtained varied between 0.999898 and 0.999928, indicating very good agreement, as can be seen from Fig. 1, and that Eq. 32 is valid from near the beginning of the reaction. These results are also supported by the comparison of the theoretical

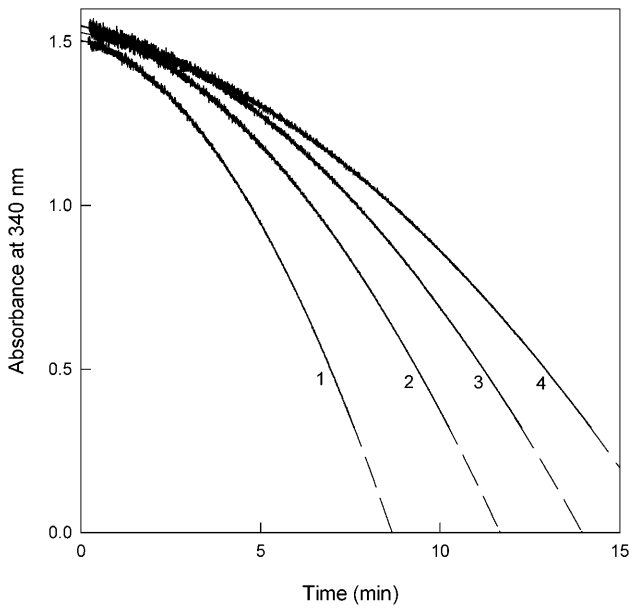

FIGURE 1 Reaction progress curves of β-NADH consumption obtained for the amplified assay of ADP by double-cycling. Experimental conditions were as indicated in the Kinetic Analysis section, including 40, 100, 180, and 400 nM of ADP for curves 1–4, respectively. The solid lines represent experimental data, and the dashed lines correspond to linear regression analysis to second-order polynomials of the reaction time, extended to the axes.

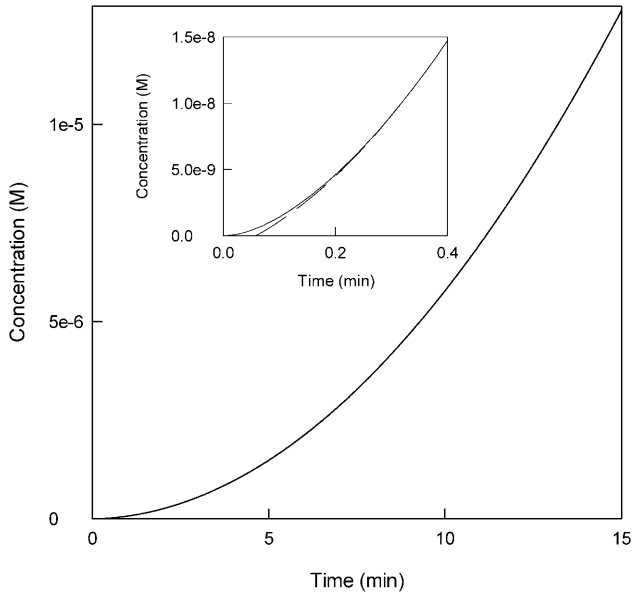

FIGURE 2 Theoretical results obtained by plotting Eqs. 15 (*solid line*) and 20 (*dashed line*) using the values experimentally obtained for k_i ($i = 1, 2, 3, 4$). Initial substrate concentration used was $X_0 = 10^{-8}$ M. The inset shows an expansion of this graph near the coordinate origin.

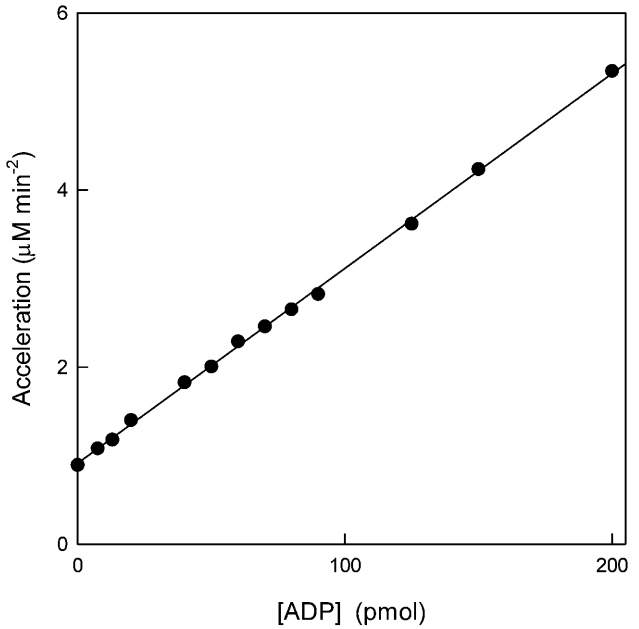

FIGURE 3 Calibration straight line for the quantification of low levels of ADP. Experimental conditions as indicated in Fig. 1. The points represent experimental data (mean of three assays), and the straight line corresponds to regression analysis plot ($y = 9.13905 \times 10^{-7} + 11.0972x$ when all concentrations are expressed in M-units, $R = 0.999139$).

results obtained by plotting Eqs. 15 and 20 using the same values for the apparent first-order rate constants k_i ($i =$ 1,2,3,4) (those experimentally obtained) and initial conditions (Fig. 2). It can be seen that the curves overlap from the very beginning of the reaction, except for ~0.2 min and at very low concentrations of the product of the reaction (P_3) (Fig. 2 *inset*), inasmuch as the difference between them is very small.

Sensitivity and linearity of the assay

Fig. 3 shows the linear dependence of the acceleration (from the term in t_2) of the process on ADP concentration (it would be the same for the quantification of ATP). Using cycling enzymes at the mentioned concentrations, good linearity was obtained over a range of 7.5–200 pmol of ADP. The lower limit of detection for ADP, calculated as a signal/noise ratio of *3*, was found to be 2.28 pmol with a relative standard deviation of 2.95% (three replicates). In this way, the continuity of the assay and the simplicity to directly obtain the kinetic parameter acceleration from progress curve data permitted the sensitivity of the assay to be increased with respect to discontinuous spectrophotometric single-cycling assays, which is usually in the range of nmol/ml (Passonneau and Lowry, 1993), attaining sensitivity levels near those achieved by bioluminescent methods (Sakakibara et al., 1999). If the double-cycling assay is compared to the self-amplifying single substrate cycle for ADP-ATP (Valero et al., 2000), under the experimental conditions here used the sensitivity of the present method has increased approximately two times. The lower limit of detection and sensitivity of double-cycling assays can still be further improved by using higher amounts of the cycling enzymes, taking into account Eq. 22. The reproducibility of the assay method was evaluated by 10 replicate measurements of solutions containing 15 nM and 40 nM ADP. The relative standard deviations were found to be 4.03% and 1.65%, respectively.

From the slope of plot in Fig. 3, we evaluated the general acceleration constant of the double enzymatic cycle, k. Under the present conditions, we obtained a value for this kinetic parameter of $11.1 \pm 9.25 \times 10^{-2}$ min^{-2}. The presence of ADP and/or ATP as contaminants can be observed, their concentration being evaluated by extrapolating to acceleration zero, according to Eq. 22. A value of 41.2 $\pm$ 1.1 pmol of ADP plus ATP was obtained under these conditions, which is similar to the value obtained by the single-cycling assay. However, the standard error committed was less in this case—possibly because this value is inside the calibration straight line, which is not the case in the single-cycling assay. Note that endogenous pyruvate and L-lactate ($P_{1,0}$ and $Q_{1,0}$) do not appear in Eq. 22.

Taking into account Eqs. 17 and 18, the concentration of both P_1 and Q_1 is continuously increasing in a linear way during the assay time. So there will be a critical time after which the performed assumptions in Kinetic Analysis are not fulfilled. In addition, in the present case it has been reported that the enzyme L-lactate dehydrogenase (E_3) shows substrate and product inhibition by pyruvate (P_1) and

L-lactate (Q_1), respectively (Stambaugh and Post, 1966). If there is any inhibition effect of P_1 and/or Q_1 on E_3, or any other kinetic effect, or if the assumptions performed are not fulfilled, the velocity of the second substrate cycle could not linearly increase in agreement with Eq. 22, and so deviations from linearity in the plot of acceleration parameter versus initial substrate concentration should be observed. In the example here illustrated, under the experimental conditions and the reaction times used, the good linearity obtained in Fig. 3 indicated that these effects were not significant. In those cases in which endogenous pyruvate and L-lactate are excessively high, further purification of enzymes involved in the system will be required to avoid undesirable nonlinearity effects.

Economical optimization

To minimize the cost of the synchronized double-cycling assay, we previously calculated the optimized price of each individual substrate cycle involved in the system taking into account the values obtained for k_{1c} and k_{2c}, as previously reported (Valero and García-Carmona, 1996). This mathematical calculation gave a price relation between the two cycles of $C_2/C_1 = 45.6$ (Sigma) and, taking into account a value of $k = 11.1\ \text{min}^{-2}$, the corresponding plots (Eqs. 26 and 30) were drawn (Fig. 4). From the coordinates of the point of intersection of the inverse first-order plot with the optimized straight line, $k^0_{1c} = 22.6\,\text{min}^{-1}$ and $k^0_{2c} = 0.5\ \text{min}^{-1}$ were obtained. Since the optimum conditions for each single enzymatic cycling assay involved in the system have been previously determined graphically, it is now very easy to calculate from the corresponding optimized straight line the smallest amount of each enzyme that needs to be used to obtain these general rate constants for each cycle and, therefore, the desired degree of acceleration. The results thus obtained were 54.08 μg/ml of pyruvate kinase, 47.18 μg/ml of hexokinase, 13.50 μg/ml of L-lactic dehydrogenase, and 18.14 μg/ml of L-lactate oxidase. The enzymatic assay carried out under these conditions provided the same cycling acceleration, as calculated by subtracting the blank (data not shown).

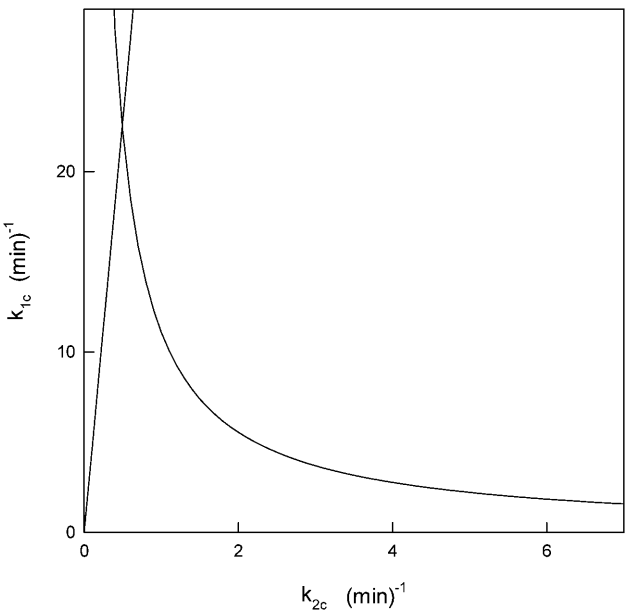

FIGURE 4 Graphical determination of the optimum conditions for the double-cycling assay using the straight line of optimization.

CONCLUDING REMARKS

The analytical equations here obtained show that product accumulation curves are second-order polynomials of the reaction time, revealing a greater sensitivity and response amplification capacity of the system than single substrate cycling. It is shown that the kinetic parameter product-accumulation acceleration is linear with the initial concentration of the recycling substrates of the first cycle, and independent of endogenous concentrations of the recycling substrates of the second cycle.

All of these conclusions allow the system to be used as a chemical amplifier in the quantitative determination of very low levels of a metabolite. However, the great increase in sensitivity increases costs substantially. Therefore, equations have been developed allowing the cost of assays to be optimized with respect to the acceleration of the process. The equations here obtained are applicable to all enzyme systems fitting reaction Scheme 1, the only restriction being that the enzymes involved in the process must follow Michaelis-Menten kinetics so that the system is linear, since the conditions referring to recycling and nonrecycling substrates depend only on the concentrations used.

The model has been illustrated by measuring nanomolar levels of ADP (and/or ATP) using the enzymes pyruvate kinase, hexokinase, L-lactic dehydrogenase, and L-lactate oxidase. This procedure has allowed us to achieve sensitivity levels near those attained by bioluminescent methods in spectrophotometric assays.

APPENDIX

$$A_1 = \frac{k_1(k_1X_0 - k_2Y_0)(k_4 - \lambda_1)}{\lambda_1^2(\lambda_1 - \lambda_2)} \tag{A1}$$

$$A_2 = k_3P_{1,0} - k_4Q_{1,0} + \frac{k_1k_3\lambda_2(k_1X_0 - k_2Y_0) - k_1k_2k_3(\lambda_1 - \lambda_2)(X_0 + Y_0)}{\lambda_1\lambda_2^2(\lambda_1 - \lambda_2)} \tag{A2}$$

$$A_3 = \frac{k_1k_2k_4(X_0 + Y_0)}{\lambda_1\lambda_2} \tag{A3}$$

$$A_4 = \frac{k_4}{\lambda_2}\left(P_{1,0} + Q_{1,0} + \frac{k_1k_4\lambda_2(k_1X_0 - k_2Y_0) + k_1k_2k_3\lambda_1(X_0 + Y_0)}{\lambda_1^2\lambda_2k_4}\right) \quad \text{(A4)}$$

$$B_1 = \frac{k_1k_3(k_1X_0 - k_2Y_0)}{\lambda_1^2(\lambda_1 - \lambda_2)} \quad \text{(A5)}$$

$$B_2 = -A_2 \quad \text{(A6)}$$

$$B_3 = \frac{k_1k_2k_3(X_0 + Y_0)}{\lambda_1\lambda_2} \quad \text{(A7)}$$

$$B_4 = \frac{k_3}{\lambda_2}\left(P_{1,0} + Q_{1,0} + \frac{k_1\lambda_2(k_1X_0 - k_2Y_0) - k_1k_2\lambda_1(X_0 + Y_0)}{\lambda_1^2\lambda_2}\right) \quad \text{(A8).}$$

The work described in this article was supported by a grant from the Dirección General de Investigación del Ministerio de Ciencia y Tecnología (Spain), Proyecto #BQU2002-01960, and by a grant from the Consejería de Ciencia y Tecnología de la Junta de Comunidades de Castilla-La Mancha, Proyecto #GC-02-032.

REFERENCES

Breckenridge, B. M. 1964. The measurement of cyclic adenylate in tissues. *Proc. Natl. Acad. Sci. USA.* 52:1580–1586.

Hammond, V. A., and D. G. Johnston. 1987. Substrate cycling between triglyceride and fatty acid in human adipocytes. *Metabolism.* 36:308–313.

Harper, J. R., and A. Orengo. 1981. The preparation of an immunoglobulin-amyloglucosidase conjugate and its quantitation by an enzyme-cycling assay. *Anal. Biochem.* 113:51–57.

Ibarguren, I., M. J. Díaz-Enrich, J. Cao, M. Fernández, R. Barcia, J. A. Villamarín, and J. I. Ramos-Martínez. 2000. Regulation of the futile cycle of fructose phosphate in sea mussel. *Comp. Biochem. Physiol. B Biochem. Mol. Biol.* 126:495–501.

Inouye, K., I. Ueno, S. Yokoyama, and T. Sakaki. 2002. Development of a synchronous enzyme-reaction for a highly sensitive enzyme immunoassay. *J. Biochem.* 131:97–105.

Johannsson, A., D. H. Ellis, D. L. Bates, A. M. Plumb, and C. J. Stanley. 1986. Enzyme amplification for immunoassays. Detection limit of one hundredth of an attomole. *J. Immunol. Methods.* 87:7–11.

Luong, J. H. T. L., A. Mulchandani, and K. B. Male. 1991. Development of a substrate recycle amplification system for L-glutamic acid assay. *Enzyme Microb. Technol.* 13:116–122.

Naka, K. 1993. Enzyme confusion. *Clin. Chem.* 39:2351.

Newsholme, E. A. 1978. Substrate cycles: their metabolic, energetic and thermic consequences in man. *Biochem. Soc. Symp.* 43:183–205.

Newsholme, E. A., R. A. J. Challiss, and B. Crabtree. 1984. Substrate cycles: their role in improving sensitivity in metabolic control. *TIBS.* 9:277–280.

Passonneau, J. V., and O. H. Lowry. 1978. Kinetics of enzymatic cycling. *In* Principles of Enzymatic Analysis. H. U. Bergmeyer, editor. Verlag Chemie, Weinheim, Germany. 86–87.

Passonneau, J. V., and O. H. Lowry. 1993. Enzymatic cycling. *In* Enzymatic Analysis. A Practical Guide. Humana Press, Totowa, NJ. 103–107, 222.

Raba, J., and H. A. Mottola. 1994. On-line enzymatic amplification by substrate cycling in a dual bioreactor with rotation and amperometric detection. *Anal. Biochem.* 220:297–302.

Sakakibara, T., S. Murakami, N. Eisaki, M. Nakajima, and K. Imai. 1999. An enzymatic cycling method using pyruvate orthophosphate dikinase and firefly luciferase for the simultaneous determination of ATP and AMP (RNA). *Anal. Biochem.* 268:94–101.

Stambaugh, R., and D. Post. 1966. Substrate and product inhibition of rabbit muscle lactic dehydrogenase heart (H_4) and muscle (M_4) isozymes. *J. Biol. Chem.* 241:1462–1467.

Valero, E., and F. García-Carmona. 1996. Optimizing enzymatic cycling assays: spectrophotometric determination of low levels of pyruvate and L-lactate. *Anal. Biochem.* 239:47–52.

Valero, E., and F. García-Carmona. 1998. A continuous spectrophotometric method based on enzymatic cycling for determining L-glutamate. *Anal. Biochem.* 259:265–271.

Valero, E., R. Varón, and F. García-Carmona. 1995. Kinetic study of an enzymic cycling system coupled to an enzymic step: determination of alkaline phosphatase activity. *Biochem. J.* 309:181–185.

Valero, E., R. Varón, and F. García-Carmona. 1997. Mathematical model for the determination of enzyme activity based on enzymatic amplification by substrate cycling. *Anal. Chim. Acta.* 346:215–221.

Valero, E., R. Varón, and F. García-Carmona. 2000. Kinetics of a self-amplifying substrate cycle: ADP-ATP cycling assay. *Biochem. J.* 350:237–243.